

## Experimental Hydrodynamics and Evolution: Function of Median Fins in Ray-finned Fishes<sup>1</sup>

GEORGE V. LAUDER<sup>2</sup> JENNIFER C. NAUEN, AND ELIOT G. DRUCKER

*Museum of Comparative Zoology, Harvard University, 26 Oxford St., Cambridge, Massachusetts 02138*

**SYNOPSIS.** The median fins of fishes consist of the dorsal, anal, and caudal fins and have long been thought to play an important role in generating locomotor force during both steady swimming and maneuvering. But the orientations and magnitudes of these forces, the mechanisms by which they are generated, and how fish modulate median fin forces have remained largely unknown until the recent advent of Digital Particle Image Velocimetry (DPIV) which allows empirical analysis of force magnitude and direction. Experimental hydrodynamic studies of median fin function in fishes are of special utility when conducted in a comparative phylogenetic context, and we have examined fin function in four ray-finned fish clades (sturgeon, trout, sunfish, and mackerel) with the goal of testing classical hypotheses of fin function and evolution. In this paper we summarize two recent technical developments in DPIV methodology, and discuss key recent findings relevant to median fin function. High-resolution DPIV using a recursive local-correlation algorithm allows quantification of small vortices, while stereo-DPIV permits simultaneous measurement of  $x$ ,  $y$ , and  $z$  flow velocity components within a single planar light sheet. Analyses of median fin wakes reveal that lateral forces are high relative to thrust force, and that mechanical performance of median fins (*i.e.*, thrust as a proportion of total force) averages 0.35, a surprisingly low value. Large lateral forces which could arise as an unavoidable consequence of thrust generation using an undulatory propulsor may also enhance stability and maneuverability. Analysis of hydrodynamic function of the soft dorsal fin in bluegill sunfish shows that a thrust wake is generated that accounts for 12% of total thrust and that the thrust generation by the caudal fin may be enhanced by interception of the dorsal fin wake. Integration of experimental studies of fin wakes, computational approaches, and mechanical models of fin function promise understanding of instantaneous forces on fish fins during the propulsive cycle as well as exploration of a broader locomotor design space and its hydrodynamic consequences.

### INTRODUCTION

It has long been recognized that the median fins of fishes (dorsal, caudal, and anal fins) play an important role in generating locomotor forces as fishes swim steadily, accelerate, and maneuver in the aquatic environment (Alexander, 1967; Gray, 1968; Gosline, 1971). But the orientations and magnitudes of these forces, the mechanisms by which they are generated, and how fish modulate median fin forces have remained largely unknown until very recently.

The major obstacle to improving our understanding of median fin function in fishes has been the difficulty of measuring *in vivo* forces generated by the fins. Analyses of terrestrial locomotor mechanics have relied heavily on direct measurements of the forces exerted by limbs on the ground (*e.g.*, Kram and Powell, 1989; Biewener, 1992; Lee *et al.*, 1999), but such an approach has only recently been attempted for aquatic animals. In large measure this is due to the difficulty of making force measurements in fluids, and to the relatively recent movement into biology of engineering approaches such as Digital Particle Image Velocimetry (DPIV) that allow fluid force measurement (Willert and Gharib, 1991; Raffel *et al.*, 1998; Stanislas *et al.*, 2000). Virtually all experimental research prior to the development of DPIV has focused on the study of me-

dian fin kinematics and on using kinematic data (occasionally with the addition of electromyographic recordings) to infer the directions of locomotor forces (Bainbridge, 1963; Fierstine and Walters, 1968; Webb and Keyes, 1981; Lauder, 1989; Jayne *et al.*, 1996; Arreola and Westneat, 1997; Gibb *et al.*, 1999; Lauder, 2000). Such methods are necessarily indirect and inferential.

The advent of DPIV as an experimental technique for quantifying both the orientation and magnitude of median-fin locomotor forces in fishes has resulted in new insights into the function and evolution of median fins which have been summarized in several recent papers (Lauder, 2000; Drucker and Lauder, 2002a; Lauder *et al.*, 2002). By directly measuring the structure of the wake resulting from fin movements, classical hypotheses about median fin function and its evolution have been tested (Liao and Lauder, 2000; Drucker and Lauder, 2001a; Nauen and Lauder, 2002a; Wilga and Lauder, 2002) and new hypotheses generated which can serve as the basis for further experimental exploration of the diversity of fin function.

The purpose of this paper is twofold. First, we outline two recent technical developments in DPIV that have occurred since the publication of our previous papers reviewing this technique. These technical improvements have particular application to the study of median fin function in fishes. Second, we summarize several of the key results that have been obtained from experimental hydrodynamic studies of median fins over the last several years.

<sup>1</sup> From the Symposium *Dynamics and Energetics of Animal Swimming and Flying* presented at the Annual Meeting of the Society for Integrative and Comparative Biology, 2–6 January 2002, at Anaheim, California.

<sup>2</sup> E-mail: Glauder@oeb.harvard.edu

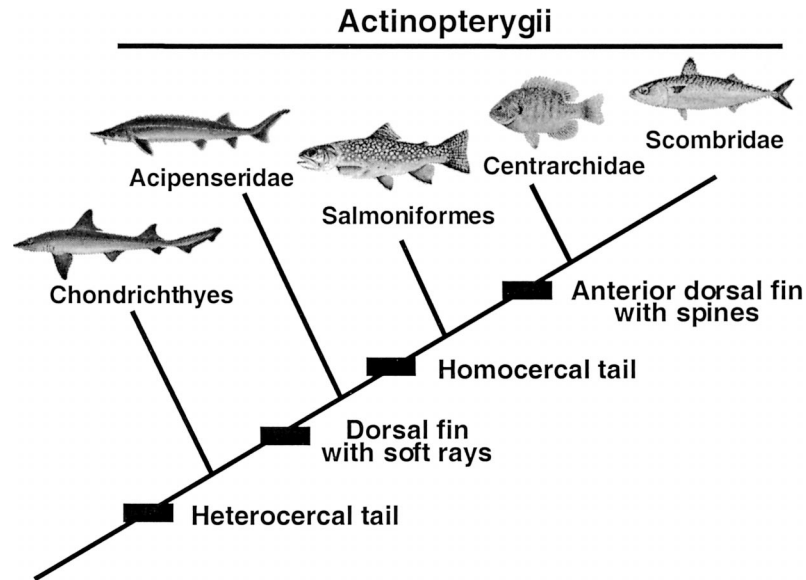


FIG. 1. Simplified phylogeny of the relationships of five taxa that have been of particular experimental interest in the analysis of median fin function in fishes. Experimental hydrodynamic analyses of fin function in sharks (*Chondrichthyes*) provide outgroup data for comparative studies of median fin function in four clades of ray-finned fishes (*Actinopterygii*). The function of the caudal fin, dorsal fin, or both fins together has been studied in each of the five taxa shown. The caudal fin is primitively heterocercal (as seen in sharks and sturgeon), while the caudal fin in more derived clades is externally symmetrical (homocercal) in shape. Most basal ray-finned fish clades possess a single dorsal fin which is supported by soft fin rays (*e.g.*, sturgeon, *Acipenseridae*, and trout, *Salmoniformes*), while derived teleost fishes typically show a dorsal fin with an anterior spiny portion and a posterior soft-rayed section (as seen in bluegill, *Centrarchidae*, and mackerel, *Scombridae*). Images of fishes modified from Scott and Crossman (1973), McClane (1974), Joseph *et al.* (1988), Paxton and Eschmeyer (1995), and Hubbs and Lagler (1958).

#### PHYLOGENETIC CONTEXT

Experimental hydrodynamic studies of median fin function in fishes are of special utility when conducted in a comparative context that allows classical evolutionary hypotheses of fin design to be examined. In this regard we have focused on obtaining experimental data on four ray-finned fish taxa which display a diversity of median fin structure (Fig. 1), and one outgroup clade (*Chondrichthyes*; Wilga and Lauder, 2002). Although the diversity of ray-finned fishes and outgroup taxa is considerable, two classical phylogenetic trends in median fin design stand out. First, basal taxa (such as *Acipenseridae*) possess heterocercal tails which are morphologically asymmetrical with an elongate upper lobe (Lauder, 2000). More derived ray-finned fishes such as *Salmoniformes*, *Centrarchidae*, and *Scombridae* (Fig. 1) possess a homocercal tail which is externally symmetrical although the internal skeleton and musculature retains plesiomorphic asymmetry.

Second, in most basal ray-finned fishes such as sturgeon and trout (Figs. 1, 2A) a single dorsal fin is present and is supported by flexible fin rays. In derived teleost fishes (*e.g.*, *Centrarchidae*, *Scombridae*; Figs. 1, 2B) the dorsal fin typically has two distinct portions. The posterior soft-rayed portion is homologous to the plesiomorphic soft dorsal fin while the anterior spiny section is an evolutionary novelty that is supported by stiffened spines with limited lateral mobility. The soft dorsal fin possesses separate erector, depressor, and in-

clinators muscles which allow considerable active control over fin conformation (Geerlink, 1974; Winterbottom, 1974; Jayne *et al.*, 1996).

In this paper we will focus on median fin function in teleost fishes; data on sturgeon and shark tail function can be found elsewhere (Liao and Lauder, 2000; Wilga and Lauder, 2002). Attempts to understand evolutionary patterns to locomotor hydrodynamics benefit considerably from broad comparative analyses, and we attempt here to provide a general overview of our approach which has focused on comparing divergent taxa containing representatives that display key morphological features of locomotor design in fishes. But this approach should be regarded as a first step to understanding the wide diversity of locomotor hydrodynamics within teleost fishes, as numerous locomotor structures and behaviors occur that have yet to be studied.

#### RECENT TECHNICAL DEVELOPMENTS

In order to investigate the function of the dorsal and caudal fins in fishes, a technique is needed that allows (1) visualization of the effect of fin motion on the water and (2) quantification of the fin wake velocity field and calculation of relevant fluid dynamic parameters such as circulation and vorticity. In previous papers we have described the technique of DPIV and how it can be applied to the study of locomotion in fishes (*e.g.*, Drucker and Lauder, 1999, 2002; Lauder, 2000; Lauder *et al.*, 2002). Briefly, fish swim in a recirculating flow tank against a current of known speed. Wa-

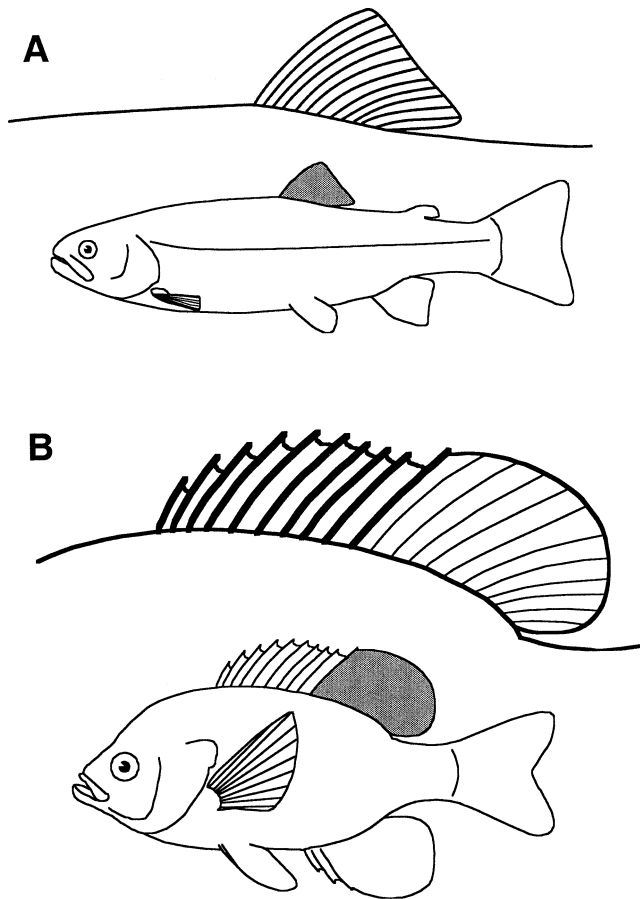


FIG. 2. Comparison of dorsal fin structure in (A) rainbow trout (*Oncorhynchus mykiss*) and (B) bluegill sunfish (*Lepomis macrochirus*). In trout the dorsal fin consists of a single relatively flexible fin supported by fin rays (indicated by thin lines in enlarged view of fin at top), while in bluegill the dorsal fin is composed of two distinct components: an anterior spiny portion supported by rigid spines (represented by thick lines), and a posterior soft-rayed section homologous to the trout dorsal fin (indicated by gray shading).

ter in the tank is seeded with small near-neutrally buoyant silver-coated particles that reflect light from a laser that has been focused into a sheet 1–2 mm thick and 10–15 cm wide. As fish swim with their fins in or just anterior to this light sheet, water movement resulting from fin oscillation is clearly seen and imaged using a high-speed video system (typically 250 frames per second). Pairs of images from these videos separated in time by 4 ms are then used to calculate a velocity vector field using standard DPIV cross-correlation algorithms (Willert and Gharib, 1991; Drucker and Lauder, 1999; Lauder, 2000). These velocity vector fields are then used to calculate fluid vorticity and circulation of identified vortices, and such calculations can be repeated for many successive 4 ms time intervals to give a picture of flow in the wake over time. In most of our previous DPIV research on fish fin function, the velocity field calculated from DPIV images was a  $20 \times 20$  matrix of vectors, yielding 400 total velocity vectors describing wake flow in an area approximately  $10 \times 10$  cm in size. Such resolution has

been sufficient to generate accurate estimates of locomotor force (Drucker and Lauder, 1999; Nauen and Lauder, 2002a), to determine how fin forces change with speed and during maneuvering behaviors (Drucker and Lauder, 2000, 2001b), and to quantify flow in the region of the caudal peduncle and tail (Lauder, 2000; Nauen and Lauder, 2001; Wilga and Lauder, 2002).

In our prior studies, velocity vectors were calculated in two or more orthogonally oriented light sheets to construct a three-dimensional picture of flow in the wake. By conducting separate experiments and reorienting the laser light sheet to illuminate flow in the *XY*, *XZ*, and *YZ* planes, and then combining the results of these separate two-dimensional analyses, we have been able to document the three-dimensional structure of vortex rings shed by fish fins and the changes in ring configuration that occur with body position and locomotor speed (Wilga and Lauder, 1999, 2000; Drucker and Lauder, 2000, 2001b; Nauen and Lauder, 2002a).

#### High resolution DPIV

Although the  $20 \times 20$  vector resolution of wake velocity fields has been sufficient for reconstructing median-fin vortex wakes to date, during routine locomotor behavior the fins of many fishes generate relatively weak vortices which are not visualized effectively at this relatively low resolution. For example, the pectoral fins of trout produce small vortices during turning and braking (Drucker and Lauder, 2002b) which require higher resolution velocity fields to accurately determine vortex structure and to calculate circulation and vorticity.

Fortunately, the advent of new processing algorithms has allowed much higher resolution imaging of the fin vortex wake. Hart (2000) introduced a recursive local-correlation algorithm which augments the standard cross-correlation DPIV processing approach. The Hart algorithm first calculates a velocity vector field using standard cross-correlation and then subdivides the initial areas of interrogation and calculates new estimates of flow velocities within each of the subdivided areas. The initial correlation is used as a predictor of correlations within each of the new subdivided areas. This procedure can be repeated by further subdividing areas of interrogation into yet smaller areas to generate a high-resolution velocity vector field which is robust to propagated processing errors (Hart, 2000).

Figure 3 shows a high-resolution two-dimensional velocity vector field obtained from the caudal fin wake in rainbow trout (*Oncorhynchus mykiss*) swimming steadily in a flow tank at 1.0 L (total body length)  $\text{sec}^{-1}$ . This vector field represents flow in an area of approximately 6 cm by 7 cm, and contains 2,100 velocity vectors in a 50 by 42 matrix. Lateral (*Z*-direction) oscillation of the tail has produced two counter-rotating centers of vorticity with a central jet flow directed posterolaterally, and this jet orientation reflects

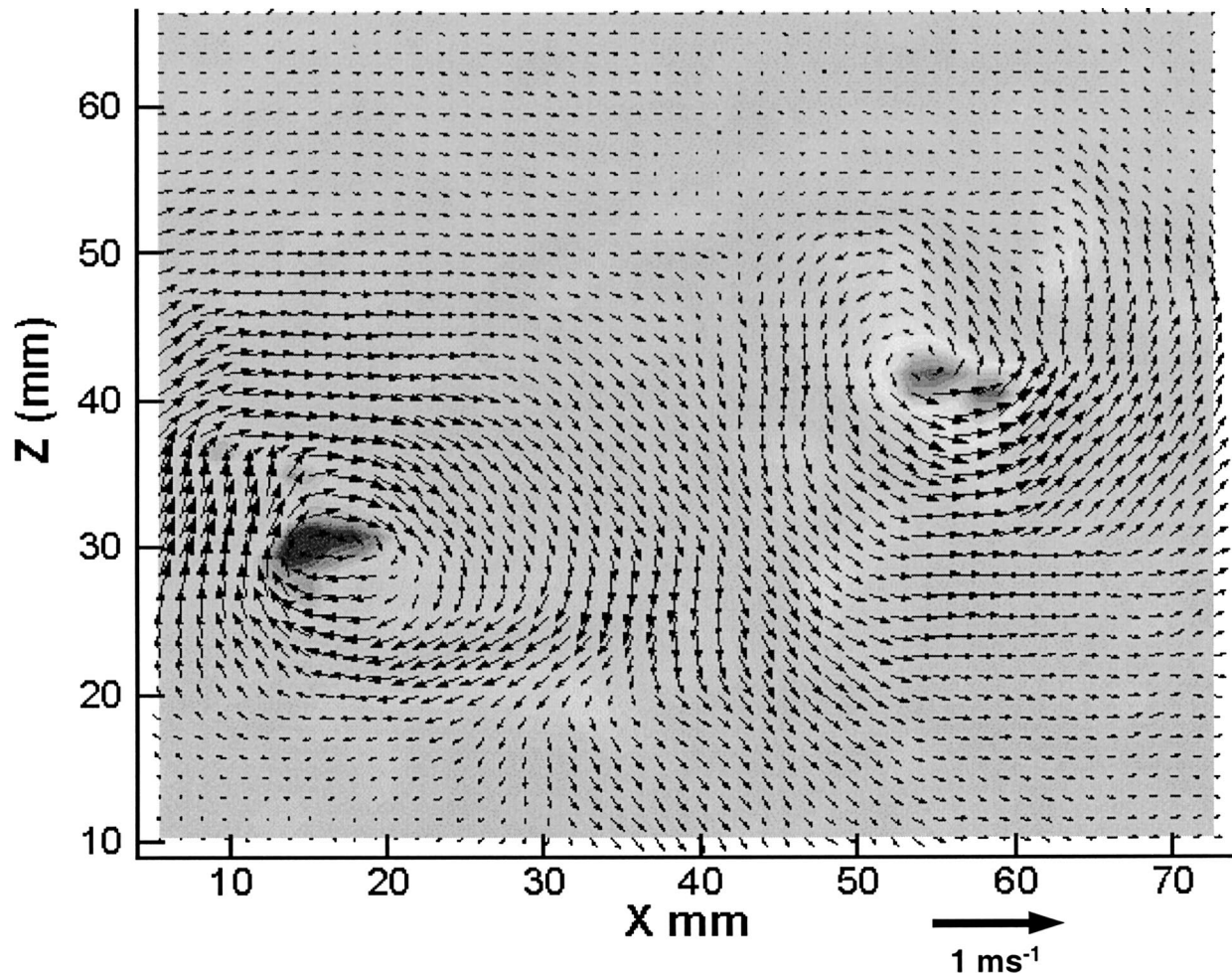


FIG. 3. Pattern of velocity vectors resulting from a high-resolution DPIV analysis in the horizontal ( $XZ$ ) plane of the wake behind the caudal fin of a freely swimming trout (*Oncorhynchus mykiss*, 19 cm total length,  $L$ ), swimming steadily at  $1.0 L \text{ sec}^{-1}$ . Freestream flow is from left to right. Over 2000 vectors are shown, and a mean downstream flow of  $19 \text{ cm sec}^{-1}$  has been subtracted from each vector to reveal tail wake vortices. Note that a single tail beat has produced two counterrotating vortices with a central jet flow directed posterolaterally. The grayscale background shows centers of fluid vorticity ( $\text{sec}^{-1}$ ) with dark cores indicating high rates of fluid rotation and the lighter gray areas reflecting low vorticity.

both thrust production (the downstream  $x$  component) and equivalently large lateral forces (the lateral  $z$  component). The vector resolution shown in Figure 3 is five times greater than our previous experimental studies of caudal fin propulsion in fishes.

#### Stereo-DPIV

One limitation of conventional DPIV analyses has been the two-dimensional representation of fluid motion in planar flow fields. Despite the possibility of examining median-fin wake geometry in up to three orthogonal light sheets, the velocity vector fields remain two-dimensional, with only two of three possible velocity components quantifiable at any instant in time. One way to improve experimental analysis of median-fin flow fields would be to measure all three components of flow velocity simultaneously. This can now be achieved using a stereo-DPIV technique (Gaydon *et al.*, 1997; Lawson and Wu, 1997; Willert, 1997; Westerweel and Oord, 2000) in which two cameras

simultaneously image flow in a 1–2 mm-thick light sheet.

Figure 4 illustrates the experimental arrangement used to accomplish stereo-DPIV. Flow in the wake of the caudal fin is shown as a vector passing through the light sheet, and this vector has components parallel to the  $X$  and  $Y$  axes within the light sheet and also a  $z$  component orthogonal to the light sheet. By arranging two cameras at oblique angles to the light sheet (Fig. 4A) and recording simultaneous images of the area of visual overlap, the  $x$ ,  $y$ , and  $z$  components of flow in that region can be calculated once a detailed calibration is performed (Nauen and Lauder, 2002b). However, when cameras are oriented at such an oblique angle to the light sheet, it is not possible to focus the cameras on the entire area of interest unless special conditions are met. Figure 4B shows that if the lens of each camera is detached from the camera body containing the CCD sensor (using a custom mounting bracket not shown in the figure), and if the plane of

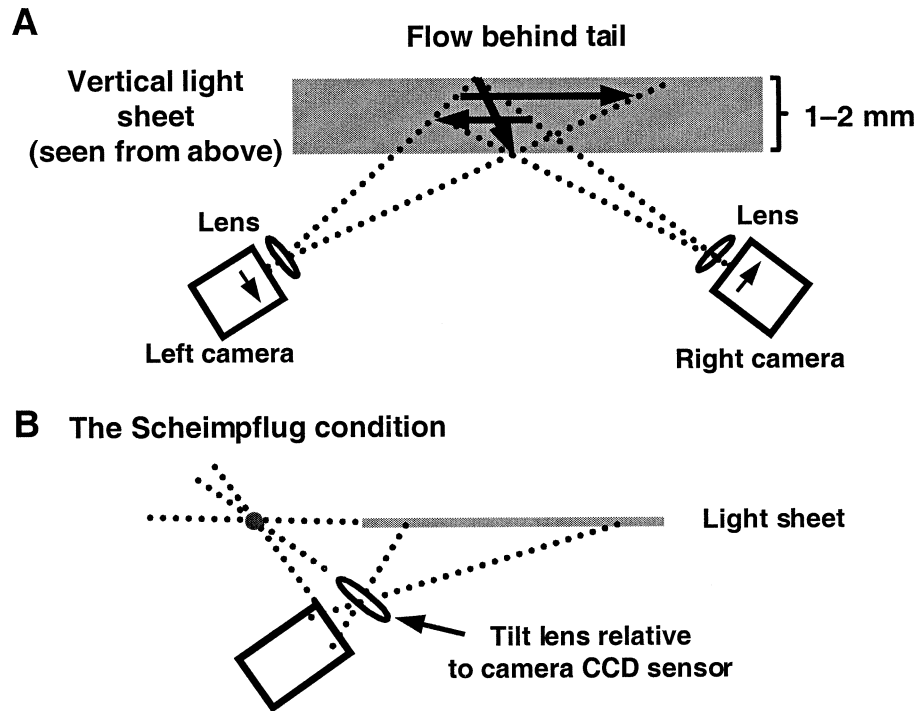


FIG. 4. Schematic diagram of the experimental arrangement of cameras and laser light sheet used to obtain stereo-DPIV data on the median fin wake of freely swimming fishes (Nauen and Lauder, 2002b). (A) Two cameras are positioned at a large ( $>90^\circ$ ) angle to each other and aimed at a vertical ( $XY$ ) light sheet 1–2 mm thick. Flow through the light sheet (shown as the obliquely oriented arrow) has two in-plane components ( $x$  and  $y$ ) and an out-of-plane component ( $z$ ). Using stereo-DPIV, all three components of flow can be imaged simultaneously. A complex calibration procedure is used to correct for distortion introduced by the camera angles and to allow calculation of the  $\Delta x$ ,  $\Delta y$ , and  $\Delta z$  flow components within the overlapping field of view of the two cameras. Arrows pointing to the left and right in the plane of the light sheet show the two-dimensional image of the true three-dimensional flow as seen by each separate camera. The small arrows located inside each camera indicate the image of flow as seen by each camera. (B) In order for the plane of the light sheet to be in focus when cameras are significantly non-orthogonal, the Scheimpflug condition must be met. When the plane of the camera sensor, the plane of the light sheet and the plane of the lens all meet in a line (shown as a large dot indicating a line perpendicular to the page), the light sheet will be in focus on the camera sensor despite the angle of the camera. Note that this requires that the camera lens be decoupled from the camera body so that the axes of the camera CCD sensor and lens can be oriented independently.

the lens, the plane of the camera CCD sensor, and the plane of the light sheet meet at a common line (the Scheimpflug condition), the full field of view will be in focus despite the angle of the camera (Raffel *et al.*, 1998; Stanislas *et al.*, 2000). The Scheimpflug condition is the principle behind viewgraph cameras and allows sharp focus despite non-orthogonal orientations between the camera and subject plane.

To demonstrate the ability of stereo-DPIV to image flow in the wake of freely swimming fishes we used two digital video cameras aligned in the Scheimpflug configuration and focused on a parasagittal ( $XY$ ) laser light sheet centered in a flow tank. Stereo sequences of DPIV images representing wake flow patterns were obtained at  $250 \text{ images sec}^{-1}$ . Trout (*Oncorhynchus mykiss*) swam steadily at  $1.2 \text{ L sec}^{-1}$  with their tail beating just upstream of the light sheet, sending vortices downstream and into view of the stereo cameras. Figure 5 shows two views of the three-dimensional flow field in the wake of the trout tail recorded with stereo-DPIV. Central jet flow through vortex rings is visible as flow to the right (positive  $Z$ ) and left (negative  $Z$ ) of the laser light sheet which is located at the  $Z = 0$  position. Alternating jet flow patterns produced

by the tail beats to each side are clearly seen. Each velocity vector shown in Figure 5 has measured  $x$ ,  $y$ , and  $z$  components which permit three-dimensional quantification of wake flow patterns.

Although the stereo-DPIV technique does not provide an instantaneous snapshot of flow within the entire wake volume, it does nonetheless represent a valuable additional experimental tool for the analysis of the wake flow patterns of swimming fishes.

#### KEY RESULTS

Two key contributions to our understanding of fish locomotion have come from *in vivo* DPIV studies on median fin function in freely swimming fishes: (1) quantification of fin force magnitudes and orientations, and (2) identification of thrust wake signatures where none was previously suspected. The first of these is relevant to the function of the caudal fin for which a thrust wake has long been recognized but force measurement difficult, while the second pertains to the dorsal fin which has not previously been suspected of generating thrust independent of the body and caudal fin. In all cases studied to date, analysis of fluid jet directions and forces necessitates study of multiple in-

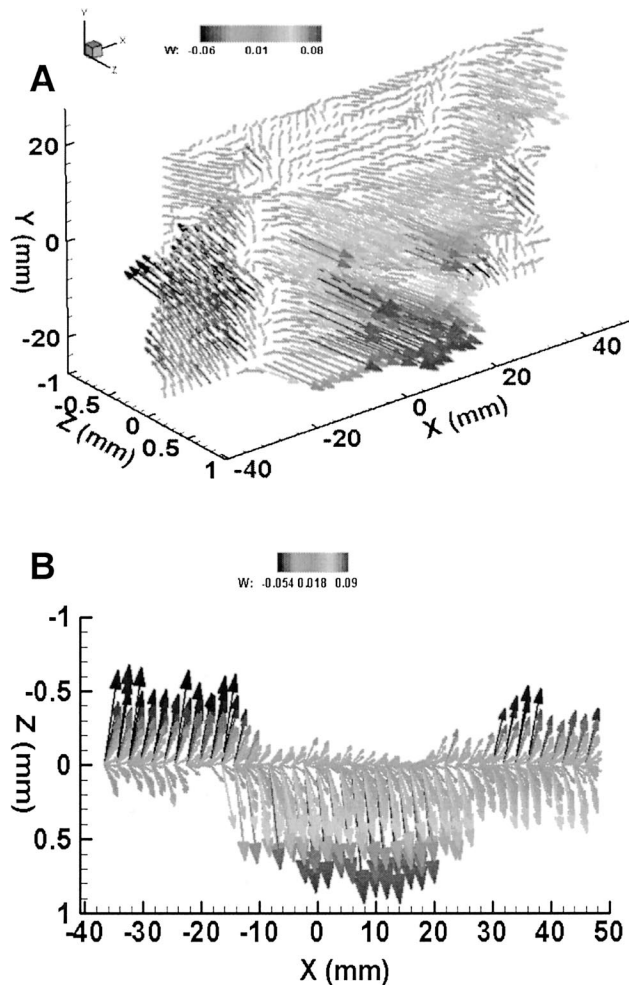


FIG. 5. Stereo-DPIV data of flow in the wake of a rainbow trout (21.5 cm long) swimming steadily at  $1.2 \text{ L sec}^{-1}$ . (A) Perspective view of 1,092 vectors showing the  $x$ ,  $y$ , and  $z$  components of flow. Flow to the left (away from the reader) is in the negative  $Z$  direction, while flow to the right (toward the reader) occurs in the positive  $Z$  direction. Mean freestream flow has not been subtracted. Vector bases are anchored at a value of 0 on the  $Z$  axis. (B) Top view looking down on the same data displayed in panel A, which clearly shows alternating jet flow originating from tail vortex rings. Scale bars indicate the  $w$  (or  $Z$ -direction) component of flow in  $\text{m sec}^{-1}$ . Positive  $X$  values increase in the downstream direction; note that the scales for the  $x$  and  $z$  components differ considerably and that the  $z$  component is greatly enlarged for clarity. More details are given in Nauen and Lauder (2002b).

dividuals and multiple fin beats to generate sufficiently large sample sizes to permit statistically based conclusions for intraspecific among-fin analyses, quantification of speed effects, interspecific comparisons, and analysis of different locomotor behaviors (e.g., Drucker and Lauder, 2001a, b; Nauen and Lauder, 2002a; Wilga and Lauder, 2000, 2002).

#### Function of the caudal fin

Comparative DPIV analyses of the function of the homocercal teleost tail show that the overall mechanical performance ( $\eta$ ) of the caudal fin is relatively low and yet similar across a wide phylogenetic range of

species. Mechanical performance is defined as the proportion of the total force generated by the tail that is thrust. For the caudal fin of bluegill sunfish (*Lepomis macrochirus*),  $\eta$  is 0.38 (data in Drucker and Lauder, 2001a). Bluegill are not known for high performance locomotion and it might be argued that taxa that swim steadily for long periods may possess a caudal fin with higher mechanical performance. Mackerel (*Scomber japonicus*) are members of the scombrid fish clade that includes tuna and bonitos and possess a forked tail (Fig. 6A). Locomotor kinematics in mackerel are similar to tuna (Donley and Dickson, 2000) and mackerel swim steadily at speeds of 1–2 body lengths per second in the field. The mechanical performance of the mackerel tail is 0.32 (Fig. 6A; Nauen and Lauder, 2002a), however, because mackerel produce a large lateral force with each tail beat. A mackerel of 23-cm fork length (FL) swimming at  $1.2 \text{ FL sec}^{-1}$  produces 11 mN thrust with each tail beat but 22 mN of lateral force. Vertical forces are small and on the order of 1 mN. The bluegill caudal fin also generates lateral forces which are nearly twice thrust force. Similarly large lateral forces relative to thrust force have been observed in trout (Drucker and Lauder, in preparation), mullet (Müller *et al.*, 1997), and danio (Wolfgang *et al.*, 1999).

It is of interest to compare the relative force magnitudes of caudal fins to previously published work on the forces generated by the pectoral fin in bluegill (Fig. 6B; Drucker and Lauder, 1999). Below speeds of about  $1.0 \text{ L sec}^{-1}$  bluegill of adult size swim exclusively with their pectoral fins, and at these speeds lateral forces exceed thrust force by approximately 25 percent. Overall pectoral fin mechanical performance  $\eta$  is 0.39, and this low value is due to the generation of relatively high lift and lateral forces.

The observed large lateral force magnitudes are surprising as locomotor efficiency would increase if fins could generate a greater proportion of thrust with each beat. At least two explanations can be adduced to account for such large lateral forces. First, large lateral forces may enhance body stability and thus may be actively produced to buffer fish against perturbations induced by destabilizing local water currents. The cylindrical body shape of most fishes may require dynamic stability mechanisms to allow control of body position (also see Webb, 1993; Weihs, 1993), and lateral forces generated by median and paired fins would serve to generate corrective moments about the center of mass. Furthermore, a locomotor design that involves large lateral force generation either by paired fins (Drucker and Lauder, 2001b) or median fins (Nauen and Lauder, 2002a) may significantly enhance maneuverability. Asymmetrical force couples resulting from unilateral caudal or pectoral fin movement would rapidly induce rotational moments and a change in heading. Under this view, large lateral forces are the result of positive selection for maneuverability.

A second perspective is that large lateral forces are an unavoidable consequence of undulatory propulsive

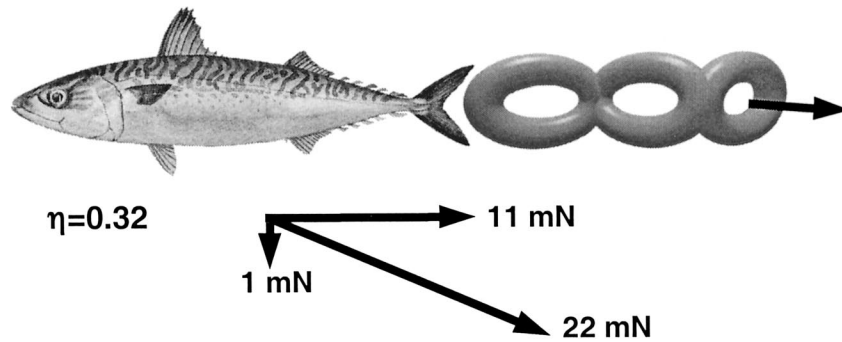
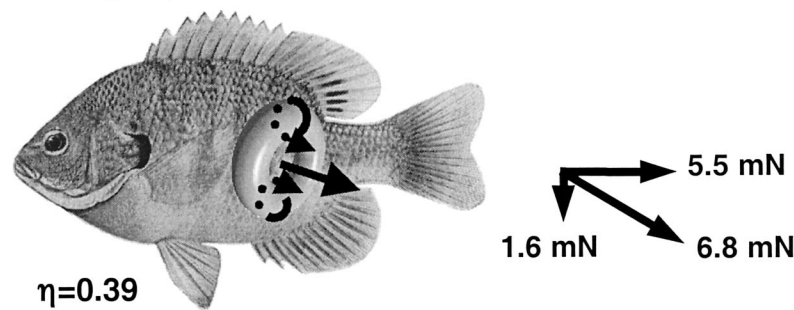
**A Mackerel: caudal fin forces at 1.2 Ls<sup>-1</sup>****B Bluegill: pectoral fin forces at 0.5 Ls<sup>-1</sup>**

FIG. 6. Summary diagram of the vortex wake produced by the tail of mackerel (A) swimming at 1.2 fork length  $\text{sec}^{-1}$ , and the pectoral fins of bluegill (B) during paired fin locomotion at 0.5 total length  $\text{sec}^{-1}$ . The mackerel tail produces a series of linked vortex rings (Nauen and Lauder, 2002a) with a central high-velocity jet through the center of each ring, indicated schematically by the arrow on the ring at far right. At low speed each beat of the pectoral fin in bluegill generates a single isolated vortex ring (Drucker and Lauder, 1999). Stroke-averaged forces are resolved into perpendicular components (thrust, lift and laterally directed force). The fins have similar mechanical performance ( $\eta$ ) averaging 0.35, due mostly to the large lateral forces generated (which exceed thrust force by a factor of 1.2 and 2.0) during each fin beat. Figures of mackerel and bluegill modified from Joseph *et al.* (1988) and Hubbs and Lagler (1958).

mechanisms and in fact are expected when a flexible propulsor is oscillated in a fluid (Lighthill, 1971, 1975). When propagated waves of bending are used to generate thrust, large lateral forces are necessarily produced and represent energy lost as a consequence of thrust generation (Carling *et al.*, 1998). Such lateral forces may be useful for maneuvering and controlling body stability, but their origin results from the physics of undulatory propulsion and not necessarily as a specific design feature of fish propulsion. The two alternatives outlined above are not mutually exclusive, and lateral forces arising from undulatory propulsion may indeed be important for maneuvering.

Finally, experimental analyses of the caudal fin have demonstrated that the caudal fin wake of fishes as diverse as sharks, sturgeon, trout, bluegill, and mackerel, shares several characteristics at odds with recent computational fluid dynamic analyses (*e.g.*, Cheng and Chahine, 2001). In all cases, vortex wake height closely approximates the height of the caudal fin, there is strong vorticity in the vertical ( $XY$ ) plane and strong tip vortices are visible in this plane, and the wake consists of clearly-defined individual vortices. One vortex is shed per tail stroke, with a complete beat generating two counterrotating vortices (Figs. 3, 5, 6) rather than

a distributed pattern of many vortices per tail stroke predicted by Cheng and Chahine (2001).

*Function of the dorsal fin*

The dorsal fin of ray-finned fishes has been implicated in a number of locomotor behaviors including steady swimming, turning, and braking (Breder, 1926; Harris, 1953; Blake, 1976, 1978; Jayne *et al.*, 1996; Arreola and Westneat, 1997; Wolfgang *et al.*, 1999; Hove *et al.*, 2001). Although very little is known about the hydrodynamic function of dorsal fins, active thrust generation during steady swimming has not been a previously documented function. We were thus surprised to find that the dorsal fin of bluegill sunfish generates a distinct thrust wake during steady locomotion with a reverse von Kármán street shed from the trailing edge of the soft dorsal fin (Fig. 7; Drucker and Lauder, 2001a). During locomotion at 1.1 L  $\text{sec}^{-1}$  the soft dorsal fin of a 21 cm bluegill produces a 9 mN thrust force, on average, accounting for 12% of the total thrust force needed to overcome drag at that speed. The bluegill soft dorsal fin is also active during turning and generates 35% of total lateral force, and has a large moment around the center of mass (Drucker and Lauder 2001a).

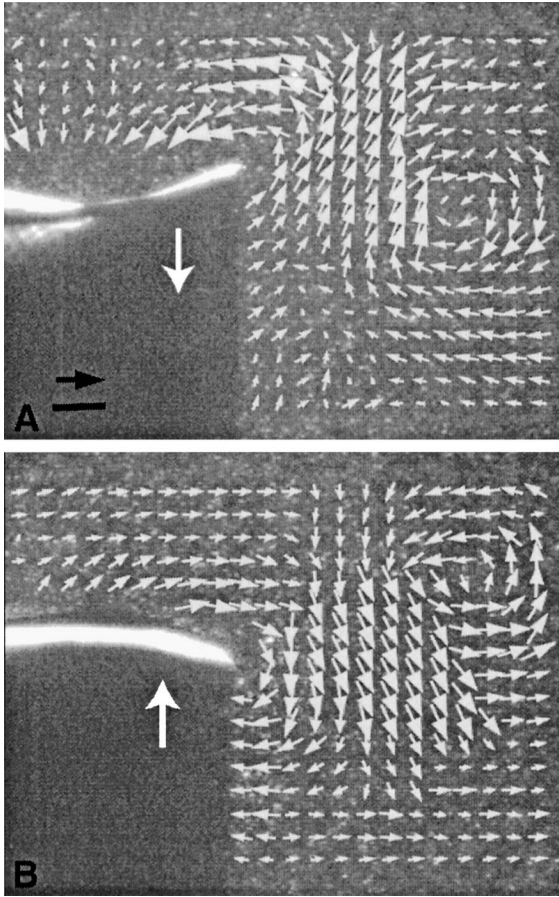


FIG. 7. The vortex wake of the soft dorsal fin in bluegill sunfish during steady locomotion at  $1.1 \text{ L sec}^{-1}$  demonstrating the thrust wake and hence active force generation by the dorsal fin. Images in (A) and (B) show horizontal-plane velocity fields separated in time by 200 m sec. Note the vortex and strong fluid jet shed downstream of the soft dorsal and the bound circulation visualized as flow near the fin. Large white arrows indicate the direction of fin motion. As shown by Drucker and Lauder (2001a), the vortex wake shed by the dorsal fin is intercepted by the tail, a potential mechanism for increasing circulation about the caudal fin. Scale bar in A is 1 cm; arrow is  $10 \text{ cm sec}^{-1}$ .

DPIV analyses of the dorsal and caudal fins together (viewed in a laser light sheet oriented to intercept both the soft dorsal trailing edge and the dorsal lobe of the caudal fin) showed that the caudal fin intercepts the vortex wake shed by the dorsal fin (Drucker and Lauder 2001a). This suggests that, as in studies of thrust enhancement in airfoils intercepting a vortex wake (Gopalkrishnan *et al.*, 1994; Anderson, 1996; Triantafyllou *et al.*, 2000), bluegill could potentially experience enhanced thrust as a consequence of increased circulation around the tail. As the tail intercepts the dorsal fin vortex wake, increased local velocity around the tail surface would increase circulation and hence thrust.

#### CONCLUSIONS

Given the enormous diversity in locomotor form and function within ray-finned fishes, and the advent

of experimental *in vivo* DPIV studies of locomotor function only within the last five years, it is clear that a great deal remains to be discovered about the function of median fins in fishes.

For example, there are currently no experimental hydrodynamic data on the function of the dorsal fin in teleost species possessing only a soft dorsal fin (Figs. 1, 2A). Only in one taxon (the bluegill sunfish) have inter-fin hydrodynamic interactions been documented, and yet this must surely be a widespread phenomenon involving potentially the dorsal, pelvic, anal, and caudal fins either all together or in some as yet unknown combination. The caudal fin of ray-finned fishes exhibits considerable diversity, and yet only the most simplistic experimental comparisons have been conducted between one species with a heterocercal tail and a select few species with homocercal tails (Fig. 1).

As quantitative flow visualization methods and analytical techniques become ever more sophisticated over the next decade, it will become easier to integrate experimental hydrodynamic data with computational analyses and mechanical models of fin function in which forces can be measured experimentally. Such integrated studies promise understanding of instantaneous forces on fish fins during the propulsive cycle as well as exploration of a broader locomotor design space and its hydrodynamic consequences.

#### ACKNOWLEDGMENTS

The research described herein and the preparation of this manuscript was supported by NSF grants IBN-9807012 and IBN-0090896. We thank Paul Webb for many discussions of fish locomotion and for lengthy and stimulating debate on the significance of wake measurements, Malcolm Gordon for the kind invitation to participate in this symposium, and the helpful comments of one referee.

#### REFERENCES

- Alexander, R. McN. 1967. *Functional design in fishes*. Hutchinson, London.
- Anderson, J. 1996. Vorticity control for efficient propulsion, MIT/WHOI, 96-02.
- Arreola, V. and M. W. Westneat. 1997. Mechanics of propulsion by multiple fins: kinematics of aquatic locomotion in the burrfish (*Chilomycterus schoepfi*). *Phil. Trans. Roy. Soc. London B* 263: 1689–1696.
- Bainbridge, R. 1963. Caudal fin and body movements in the propulsion of some fish. *J. Exp. Biol.* 40:23–56.
- Biewener, A. A. (ed.) 1992. *Biomechanics—structures and systems. A practical approach*. Oxford Univ. Press, Oxford.
- Blake, R. W. 1976. On seahorse locomotion. *J. Mar. Biol. Ass. U.K.* 56:939–949.
- Blake, R. W. 1978. On balistiform locomotion. *J. Mar. Biol. Ass. U.K.* 58:73–80.
- Breder, C. M. 1926. The locomotion of fishes. *Zoologica N. Y.* 4: 159–256.
- Carling, J. C., T. L. Williams, and G. Bowtell. 1998. Self-propelled anguilliform swimming: Simultaneous solution of the two-dimensional Navier-Stokes equations and Newton's laws of motion. *J. Exp. Biol.* 201:3143–3166.
- Cheng, J.-Y. and G. L. Chahine. 2001. Computational hydrodynamics of animal swimming: Boundary element methods and three-



- dimensional vortex wake structure. *Comparative Biochemistry and Physiology* 131:51–60.
- Donley, J. and K. A. Dickson. 2000. Swimming kinematics of juvenile kawakawa tuna (*Euthynnus affinis*) and chub mackerel (*Scomber japonicus*). *J. Exp. Biol.* 203:3103–3116.
- Drucker, E. G. and G. V. Lauder. 1999. Locomotor forces on a swimming fish: Three-dimensional vortex wake dynamics quantified using digital particle image velocimetry. *J. Exp. Biol.* 202:2393–2412.
- Drucker, E. G. and G. V. Lauder. 2000. A hydrodynamic analysis of fish swimming speed: wake structure and locomotor force in slow and fast labriform swimmers. *J. Exp. Biol.* 203:2379–2393.
- Drucker, E. G. and G. V. Lauder. 2001a. Locomotor function of the dorsal fin in teleost fishes: Experimental analysis of wake forces in sunfish. *J. Exp. Biol.* 204:2943–2958.
- Drucker, E. G. and G. V. Lauder. 2001b. Wake dynamics and fluid forces of turning maneuvers in sunfish. *J. Exp. Biol.* 204:431–442.
- Drucker, E. G. and G. V. Lauder. 2002a. Experimental hydrodynamics of fish locomotion: Functional insights from wake visualization. *Integr. Comp. Biol.* 42:243–257.
- Drucker, E. G. and G. V. Lauder. 2002b. Wake dynamics and locomotor function in fishes: Interpreting evolutionary patterns in pectoral fin design. *Integr. Comp. Biol.* 42:997–1008.
- Fierstine, H. L. and V. Walters. 1968. Studies in locomotion and anatomy of scombrid fishes. *Mem. So. Cal. Acad. Sci.* 6:1–31.
- Gaydon, M., M. Raffel, C. Willert, M. Rosengarten, and J. Kompenhans. 1997. Hybrid stereoscopic particle image velocimetry. *Exp. Fluids* 23:331–334.
- Geerlink, P. J. 1974. Joints and muscles of the dorsal fin of *Tilapia nilotica* L. (Fam. Cichlidae). *Neth. J. Zool.* 24:279–290.
- Gibb, A. C., K. A. Dickson, and G. V. Lauder. 1999. Tail kinematics of the chub mackerel *Scomber japonicus*: Testing the homocercal tail model of fish propulsion. *J. Exp. Biol.* 202:2433–2447.
- Gopalkrishnan, R., M. S. Triantafyllou, G. S. Triantafyllou, and D. Barrett. 1994. Active vorticity control in a shear flow using a flapping foil. *J. Fluid Mech.* 274:1–21.
- Gosline, W. A. 1971. *Functional morphology and classification of teleostean fishes*. Univ. of Hawaii Press, Honolulu.
- Gray, J. 1968. *Animal locomotion*. Weidenfeld and Nicolson, London.
- Harris, J. E. 1953. Fin patterns and mode of life in fishes. In S. M. Marshall and A. P. Orr (eds.), *Essays in marine biology*, pp. 17–28. Oliver and Boyd, Edinburgh.
- Hart, D. P. 2000. Super-resolution PIV by recursive local-correlation. *J. Visualiz.* 3:187–194.
- Hove, J. R., L. M. O'Bryan, M. S. Gordon, P. W. Webb, and D. Weihs. 2001. Boxfishes (Teleostei: Ostraciidae) as a model system for fishes swimming with many fins: kinematics. *J. Exp. Biol.* 204:1459–1471.
- Hubbs, C. L. and K. F. Lagler. 1958. *Fishes of the great lakes region*. Univ. of Michigan Press, Ann Arbor.
- Jayne, B. C., A. Lozada, and G. V. Lauder. 1996. Function of the dorsal fin in bluegill sunfish: Motor patterns during four locomotor behaviors. *J. Morph.* 228:307–326.
- Joseph, J., W. Klawe, and P. Murphy. 1988. *Tuna and billfish: Fish without a country*. Inter-American Tropical Tuna Commission, La Jolla.
- Kram, R. and A. J. Powell. 1989. A treadmill-mounted force platform. *J. Appl. Physiol.* 67:1692–1698.
- Lauder, G. V. 1989. Caudal fin locomotion in ray-finned fishes: Historical and functional analyses. *Amer. Zool.* 29:85–102.
- Lauder, G. V. 2000. Function of the caudal fin during locomotion in fishes: kinematics, flow visualization, and evolutionary patterns. *Amer. Zool.* 40:101–122.
- Lauder, G. V., E. G. Drucker, J. Nauen, and C. D. Wilga. 2002. Experimental hydrodynamics and evolution: caudal fin locomotion in fishes. In V. Bels, J.-P. Gasc, and A. Casinos (eds.), *Vertebrate biomechanics and evolution*, pp. 117–135. BIOS Scientific Publishers, Oxford.
- Lawson, N. J. and J. Wu. 1997. Three-dimensional particle image velocimetry: Experimental error analysis of a digital angular stereoscopic system. *Meas. Sci. Tech.* 8:1455–1464.
- Lee, D., J. Bertram, and R. Todhunter. 1999. Acceleration and balance in trotting dogs. *J. Exp. Biol.* 202:3565–3573.
- Liao, J. and G. V. Lauder. 2000. Function of the heterocercal tail in white sturgeon: Flow visualization during steady swimming and vertical maneuvering. *J. Exp. Biol.* 203:3585–3594.
- Lighthill, J. 1971. Large-amplitude elongated body theory of fish locomotion. *Proc. Roy. Soc. London B.* 179:125–138.
- Lighthill, J. 1975. *Mathematical biofluidynamics*. Society for Industrial and Applied Mathematics, Philadelphia.
- McClane, A. J. 1974. *McClane's field guide to freshwater fishes of north america*. Henry Holt and Co., New York.
- Müller, U. K., B. Van den Heuvel, E. J. Stamhuis, and J. J. Videler. 1997. Fish foot prints: morphology and energetics of the wake behind a continuously swimming mullet (*Chelon labrosus* Risso). *J. Exp. Biol.* 200:2893–2906.
- Nauen, J. C. and G. V. Lauder. 2001. Locomotion in scombrid fishes: visualization of flow around the caudal peduncle and finlets of the chub mackerel *Scomber japonicus*. *J. Exp. Biol.* 204:2251–2263.
- Nauen, J. C. and G. V. Lauder. 2002a. Hydrodynamics of caudal fin locomotion by chub mackerel *Scomber japonicus* (Scombridae). *J. Exp. Biol.* 205:1709–1724.
- Nauen, J. C. and G. V. Lauder. 2002b. Quantification of the wake of rainbow trout (*Oncorhynchus mykiss*) using three-dimensional stereoscopic digital particle image velocimetry. *J. Exp. Biol.* 205:3271–3279.
- Paxton, J. R. and W. N. Eschmeyer. 1995. *Encyclopedia of fishes*. Academic Press, San Diego.
- Raffel, M., C. Willert, and J. Kompenhans. 1998. *Particle image velocimetry: A practical guide*. Springer-Verlag, Heidelberg.
- Scott, W. B. and E. J. Crossman. 1973. *Freshwater fishes of Canada*. Fisheries Research Board of Canada, Ottawa.
- Stanislas, M., J. Kompenhans, and J. Westerweel. (eds.) 2000. *Particle image velocimetry: Progress toward industrial application*. Kluwer Academic, Dordrecht.
- Triantafyllou, M. S., G. S. Triantafyllou, and D. K. P. Yue. 2000. Hydrodynamics of fishlike swimming. *Ann. Rev. Fluid Mech.* 32:33–53.
- Webb, P. W. 1993. Is tilting behavior at low speed swimming unique to negatively buoyant fish? Observations on steelhead trout, *Oncorhynchus mykiss*, and bluegill, *Lepomis macrochirus*. *J. Fish Biol.* 43:687–694.
- Webb, P. W. and R. S. Keyes. 1981. Division of labor between median fins in swimming dolphin (Pisces: Coryphaenidae). *Copeia* 1981:901–904.
- Weihs, D. 1993. Stability of aquatic animal locomotion. *Cont. Math.* 141:443–461.
- Westerweel, J. and J. v. Oord. 2000. Stereoscopic PIV measurements in a turbulent boundary layer. In M. Stanislas, J. Kompenhans, and J. Westerweel (eds.), *Particle image velocimetry: Progress toward industrial application*, pp. 459–478. Kluwer Academic, Dordrecht.
- Wilga, C. D. and G. V. Lauder. 1999. Locomotion in sturgeon: Function of the pectoral fins. *J. Exp. Biol.* 202:2413–2432.
- Wilga, C. D. and G. V. Lauder. 2000. Three-dimensional kinematics and wake structure of the pectoral fins during locomotion in leopard sharks *Triakis semifasciata*. *J. Exp. Biol.* 203:2261–2278.
- Wilga, C. D. and G. V. Lauder. 2002. Function of the heterocercal tail in sharks: Quantitative wake dynamics during steady horizontal swimming and vertical maneuvering. *J. Exp. Biol.* 205:2365–2374.
- Willert, C. 1997. Stereoscopic digital particle image velocimetry for application in wind tunnel flows. *Meas. Sci. Tech.* 8:1465–1479.
- Willert, C. E. and M. Gharib. 1991. Digital particle image velocimetry. *Exp. Fluids* 10:181–193.
- Winterbottom, R. 1974. A descriptive synonymy of the striated muscles of the Teleostei. *Proc. Acad. Nat. Sci. Phil.* 125:225–317.
- Wolfgang, M. J., J. M. Anderson, M. Grosenbaugh, D. Yue, and M. Triantafyllou. 1999. Near-body flow dynamics in swimming fish. *J. Exp. Biol.* 202:2303–2327.